Observation of Tsunami Damage to Coastal Forest Using Middle Spatial Resolution Satellite Data

Observation of Tsunami Damage to Coastal Forest Using Middle Spatial Resolution Satellite Data

(Observation of tsunami damage to coastal forest by satellite)

Shimpei INOUE[1] and Chinatsu YONEZAWA[1]

[1]Graduate School of Agricultural Science, Tohoku University, Sendai, JAPAN
1-1 Amamiya-machi, Tsutsumidori, Aoba-ku, Sendai, Miyagi 981-8555, JAPAN
Tel: 81-22-717-8661 Fax:81-22-717-9542

Corresponding Author: Shimpei Inoue
e-mail: shinpei.inoue@nrr.meitetsu.co.jp

Keywords:the Great East Japan Earthquake, remote sensing, image analysis, disaster monitoring, NDVI, akagare

Received 10 November 2014; accepted 7 May 2015

Abstract

The coastal forest of the northeast region of Japan's Honshu island was seriously damaged by the tsunami caused by the Great East Japan Earthquake on 11 March 2011. In this study, we examined the possibility of identifying the damage level of the coastal forest using middle spatial resolution satellite data ALOS/AVNIR-2 and TERRA/ASTER. Two types of damage, direct damage immediately after the tsunami and 'Akagare' (red withered) damage that progress after the tsunami, were investigated. Using unsupervised classification, we classified the damage to the coastal forest by the tsunami into four stages. The level of damage by 'Akagare' was estimated using the NDVI and its distributions are revealed in this paper.

Introduction

Coastal forest is an effective protection against tsunamis and other natural disasters, such as tidal waves and typhoons (Tanaka 2009). In the 2004 Indian Ocean Tsunami, mangroves greatly contributed to a decrease in tsunami power in some regions that were hit by the tsunami (Kathiresan et al. 2005, Olwing et al. 2007, Tanaka et al. 2007, Yanagisawa et al. 2009). However, coastal forests cannot completely protect against tsunamis. In the case of huge tsunamis, coastal forests can be uprooted and cause lethal damage to the hinterland and thus result in large amounts of rubble (Tanaka 2009).

A huge tsunami caused by the Great East Japan Earthquake on 11 March 2011, seriously damaged a large coastal area of the northeast region of Japan. Fallen trees, washing away, and inundation caused by direct impact of the tsunami were confirmed immediately after the earthquake. Furthermore, additional tsunami impacts on the trees have emerged, over time, such as 'Akagare', a phenomenon where plant leaves turn reddish brown and wither away. The main reasons for 'Akagare' are generally considered to be infectious diseases and increase in salt concentration in the soil.

The purpose of this study is to investigate the possibility of using middle spatial resolution satellite data to estimate tsunami damage to coastal forests. The coastal forest damage inflicted by tsunamis has been assessed using high spatial resolution data (Koshimura 2007). Further, the large-scale damage inflicted by tsunamis has been analyzed using middle spatial resolution satellite data (Belward et al. 2007, Kouchi et al. 2007, Sirikulchayanon et al. 2008). However, tsunami damage to coastal forests has not yet been analyzed using middle spatial resolution satellite data.

In this study, we examined two types of damage. One is the direct damage immediately after the tsunami, such as fallen and washed away trees. The other is the 'Akagare' progressive damage, which was confirmed over time. To determine direct tsunami damage, we analyzed ALOS/AVNIR-2 data, and extracted coastal forest using the unsupervised classification technique. To determine the 'Akagare'

damage, we analyzed TERRA/ASTER data obtained after the earthquake. The decreases in vegetable activation were estimated from Normalized Difference Vegetation Index (NDVI) computation.

Test site and data

A coastal area of Sendai seriously damaged by the tsunami was selected as the investigation area. Sendai is located in northeast Japan. A coastal forest approximately 650 m wide extended from the seashore before the disaster. The majority of the coastal forest trees were *Pinus*. Figure 1 shows the analysis area for this study (38.1926–38.2505N, 140.9140–141.0210E).

Two areas were set up. An aerial photograph (Figure 2) shows that Area 1 (38.2367–38.2376N, 140.9917–140.9925E) did not sustain 'Akagare' damage, whereas Area 2 (38.2357–38.2367N, 140.9938–140.9949E) was seriously damaged. A ground survey conducted on 9 November 2011 confirmed both direct tsunami damage and 'Akagare' damage.

Two series of Middle Spatial Resolution Satellite Data, ALOS/AVNIR-2 and TERRA/ASTER/VNIR were analyzed. AVNIR-2 data were obtained on 25 December 2006 and 19 March 2011, before and after the tsunami, respectively. ALOS completed its operation in May 2011. ASTER/VNIR data were obtained after the tsunami on 19 March 2011, 9 June 2011, and 23 November 2011. AVNIR-2 provides multi-spectral 10-m resolution images with 70-km swath width. ASTER/VNIR provides multi-spectral 15-m resolution images with 60-km swath width.

Aerial photographs were used as reference data. The aerial photos from the Geospatial information Authority of Japan (GSI) were taken on 12 March and 26 May 2011. A ground survey was conducted on 9 November 2011.

Methodology

1. Extraction of direct tsunami damage immediately after the tsunami

NDVI was calculated as follows:

$$NDVI = (NIR - RED) / (NIR + RED) \times Gn + Of \quad (1)$$

Here, Gn is gain and Of is the offset. One hundred was applied for both gain and offset. NIR corresponds to the near infrared band and RED corresponds to the red band.

Unsupervised classification was applied to the dataset including original data of the AVNIR-2 4 bands and that of the computed NDVI band. In this study, the ISODATA clustering method was used for unsupervised classification. The ISODATA clustering method is classification method that creates clusters automatically from the initial condition. Test area is classified into thirty classes with the unsupervised classification, and one of these classes is corresponded with vegetation. Coastal forest is identified from vegetation class.

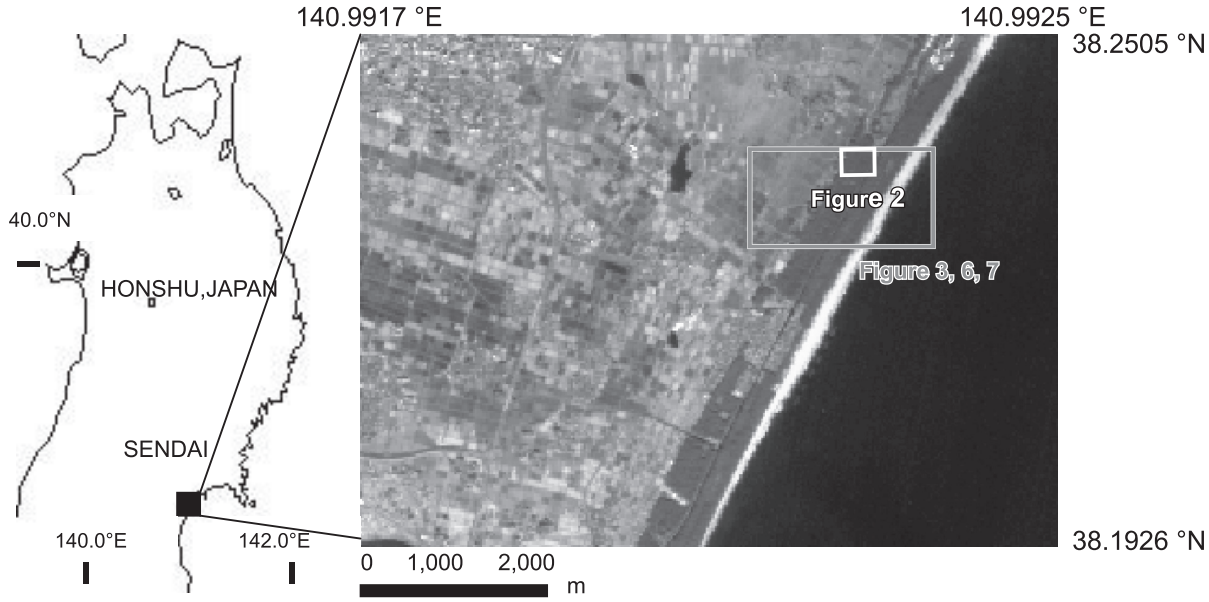

Figure 1. ALOS AVNIR-2 image of the Sendai area obtained on 25 December 2006. Color composite is false color. The white rectangle corresponds to the aerial photograph shown in Figure 2. The magenta rectangle corresponds to the area shown in Figures 3, 6, and 7.

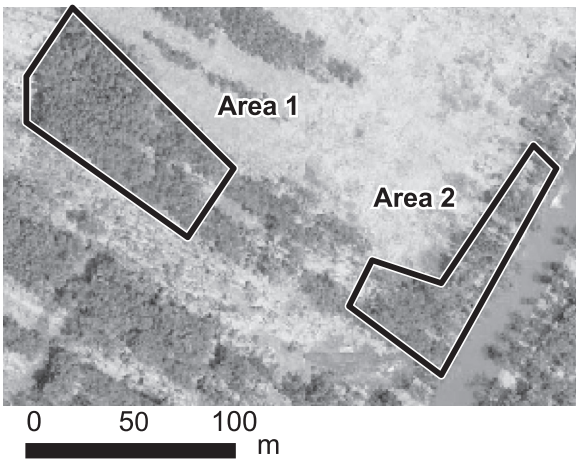

Figure 2. Aerial photograph acquired on 26 May 2011 by the Geospatial Information Authority of Japan. Area 1 corresponds to the area where 'Akagare' damage was not found. Area 2 is a seriously 'Akagare' damaged area.

The damage conditions of coastal forest after the tsunami were categorized with unsupervised classification. The coastal area in the AVNIR-2 data obtained on 19 March 2011 was classified into 30 classes. In order to classify vegetation coverage in the after-tsunami image, the non-vegetation area identified in the before-tsunami image was removed, because the removal of the non-target area decreases the errors in classification (Taguchi et al. 2003). We evaluated the classification results and compared them with the ground survey data.

2. Extraction of "Akagare" damage

NDVI of the three ASTER data were calculated using Equation (1). One hundred and twenty five was applied for both gain and offset. In this study, the NDVI were subtracted from each other to correct for reflectance between datasets easily. We call these data 'NDVI differences data'.

19 March – 9 June NDVI differences data : 19 March NDVI – 9 June NDVI (2)

9 June – 23 Nov NDVI differences data : 9 June NDV – 23 Nov NDVI (3)

19 March – 23 Nov NDVI differences data : 19 March NDVI – 23 Nov NDVI (4)

The relationship between 'Akagare' damage and decreases in NDVI was examined.

Results and Discussion

1. Extraction of direct tsunami damage

Figure 3(*a*) shows the identified vegetation area from unsupervised classification of the test site before the tsunami. One classification corresponds to vegetation area. The coastal forest is the dominant type of vegetation in the vegetation area.

In the after-tsunami image, visual interpretation with aerial photograph, four categories of damaged coastal forest were identified from unsupervised classification: remaining undamaged trees (No damage); remaining but fallen trees (Damage); removed trees and inundated land (Inundation); and removed trees with the land left bare (Bare land). These categories are shown in figure 3(*b*). Error matrices were used to assess the classification accuracy. An aerial photograph was used for reference. The overall accuracy, random 200 points corresponding, was 79.50 %, with Kappa statistics of 0.6387.

The spectral reflectance of the four identified damage categories is shown in Figure 4. The digital number of each category is the average of all pixel data in the analysis area shown in Figure 1. The digital numbers of the 'No damage' and the 'Damage' classes are high in band 4 (NIR) and low in band 3 (RED). These characteristics correspond to vegetation. The 'No damage' class shows a larger difference in the digital number between band 3 and band 4 than the 'Damage' class. A larger difference between the digital number of band 3 and band 4 indicates a larger NDVI. The digital numbers of the 'Inundation' class are low in band 3 and band 4. The 'Inundation' class corresponds to an area where coastal forest was removed and the land was inundated, so the spectral reflectance in this area is similar to that of water. The digital numbers of the 'Bare land' class are high in all bands, which can be explained by the influence of soil.

Some misclassifications are confirmed by visual interpretation. One reason for misclassifications is that the 'No damage' and 'Damage' classes show similar spectral reflectance characteristics. We defined the 'Damage' class as the area of fallen trees that remain in site, so this area contains trees in different conditions. It includes fallen trees with and without leaves. The fallen trees with leaves show similar characteristics to trees in the 'No damage' class, and fallen trees with no leaves show similar characteristics to the 'Bare land' class and the 'Inundation' class, which could lead to misclassification.

The classification results were compared with ground survey data. In figure 3(*c*), three purple

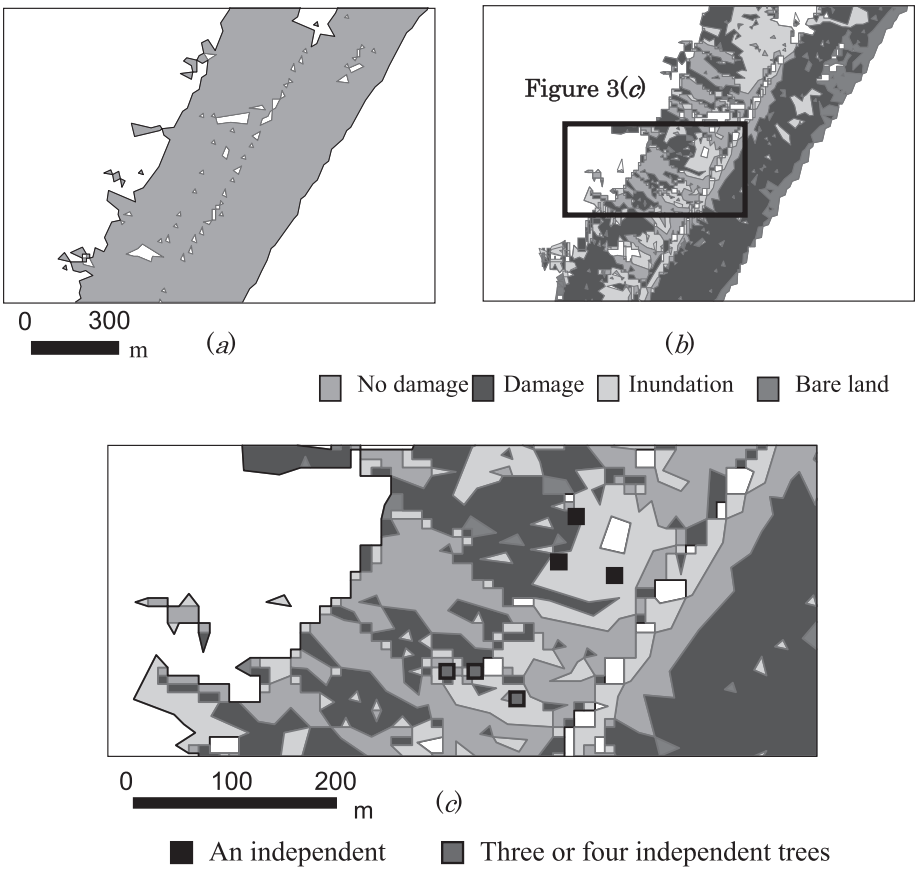

Figure 3. Classification image of the coastal forest area (*a*) before the tsunami, (*b*) after the tsunami, and (*c*) expanded image of the rectangular area denoted (*b*). The rectangular area in (*b*) corresponds to the area shown in (*c*)

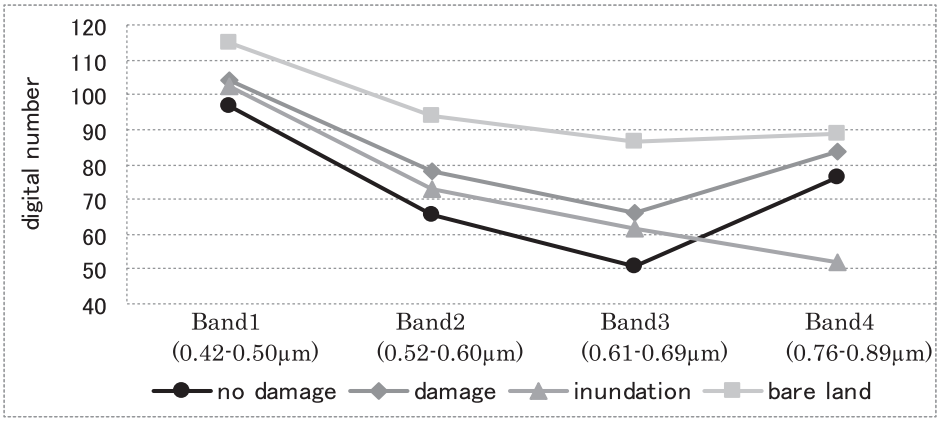

Figure 4. Spectral reflectance characteristics of the four damage categories.

squares show points where an undamaged tree stood independently. Three blue squares show points where a group of three or four undamaged trees stood independently. Two of three independent undamaged trees were classified to the 'Inundation' class rather than, the 'No damage' class. On the other hand, all of the groups of trees were correctly classified in the 'No damage' class. The mixel problem may cause misclassification of independent trees. Grouping of trees may help to avoid this problem. A mixel is a pixel that contains more than one category. The mixel problem is prominent in low spatial resolution satellites. ALOS/AVNIR-2 is a middle spatial resolution satellite with 10-m spatial resolution, which is considered insufficient for precise classification of the condition of an independent tree.

2. Extraction of 'Akagare' damage

The relation between 'Akagare' damage and decrease in NDVI was examined. The 19 March-9 June NDVI differences data for the area with no 'Akagare' damage (Area 1) and the area with extensive 'Akagare' damage (Area 2) are shown in Figure 5. A paired F-test with a 95% confidence interval showed no difference in dispersion between Area 1 and Area 2. Next, a single t-test with a 95% confidence interval that assumed same dispersion showed the average of Area 2 is larger than that of Area 1. Therefore, the decrease in NDVI in Area 2 is larger than that in Area 1. Three factors are considered as the reason decreasing NDVI. The first possible factor is seasonal change in vegetation activation. Vegetation activation is generally high in summer and low in winter, so NDVI usually increases in summer and decreases in winter. However, the predominant tree species in the target area is *Pinus*. Since *Pinus* is an evergreen tree, it would not exhibit such a seasonal change in vegetation activation. If the vegetation activation changed, the NDVI in the period from 19 March to 9 June would increase. The second possible factor for NDVI decrease is the occurrence of a large-scale natural disaster. However, such a disaster did not happen during the observation period (19 March to 23 November) at the test site. Visual interpretation of ASTER data indicates neither large-scale reduction in coastal forest nor changes in land use. The third possible reason is 'Akagare' damage. Because of the low probabilities of other factors, we infer that the decreases in NDVI were caused by 'Akagare' overwhelmingly. There is a relationship between NDVI decrease and 'Akagare' damage.

A composite image of 19 March-9 June NDVI differences data and 9 June-23 Nov NDVI differences data is shown in Figure 6. The transition of area showing an NDVI decrease from 19 March to 23 November is also shown. The area showing a NDVI decrease in trees corresponds to the area classified as the 'No damage' area in the after tsunami classification.

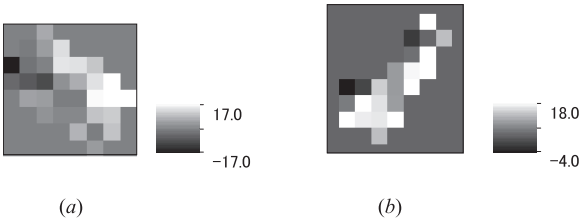

Figure 5. 19 March-9 June NDVI differences data for (*a*) Area 1 and (*b*) Area 2 shown in Figure 2.

The area that is not black in Figure 6 corresponds to the area of coastal forest identified from the ALOS/AVNIR-2 image classification before the tsunami. In Figure 6, the green area shows that the 19 March-9 June NDVI differences data are greater than 0 and the 9 June-23 Nov NDVI differences data are equal to or lower than 0, indicating a remarkable decrease from 19 March to 9 June. The magenta area shows that the 19 March-9 June NDVI differences data are equal to or lower than 0 and the 9 June-23 Nov NDVI differences data are greater than 0, indicating a remarkable decrease from 9 June to 23 November. The white area indicates that the 19 March-9 June NDVI differences data and the 9 June-23 Nov NDVI differences data are higher than 0, indicating a decrease from 19 March to 23 November, via 9 June. An area showing NDVI decrease from 19 March to 9 June was identified. This indicates the occurrence of 'Akagare' damage on 9 June. From 9 June to 23 November, the NDVI decreasing area spread. This could be interpreted as expanding of 'Akagare' damage during this term. 'Akagare' damage in Area 2 is confirmed by aerial photographs. Most of Area 2 is occupied by white pixels, which indicates that the decrease in NDVI had begun before 9 June. White pixels are also found in Area 1, where 'Akagare' damage was not found on 26 May. The mixel problem could possibly explain the presence of white pixels in Area 1. There is a possibility that 'Akagare' damage in Area 1 was not identifiable from the aerial photograph. The ASTER data was acquired 14 days later than the aerial photograph observation, and 'Akagare' damage could have occurred during this term.

Levels of NDVI decrease were estimated by setting up a threshold for the 19 March-23 Nov NDVI differences data (Figure 7). The average of 19 March-23 Nov NDVI differences data in the investigation area is -2.59418. In NDVI differences data, a value close to the average indicates a slight change in NDVI. A value larger than the average indicates a decrease in NDVI, a value smaller than the average indicates an increase in NDVI. The area classified as 'No damage' immediately after the tsunami shows values that exceed the average by far. This means that the area with decreasing NDVI spread wide. A decrease in NDVI is found in Area 1 and Area 2. However, the decrease in Area 2 is larger than that in Area 1.

The area closest to the sea was severely damaged. There are pixels that indicate a different class from

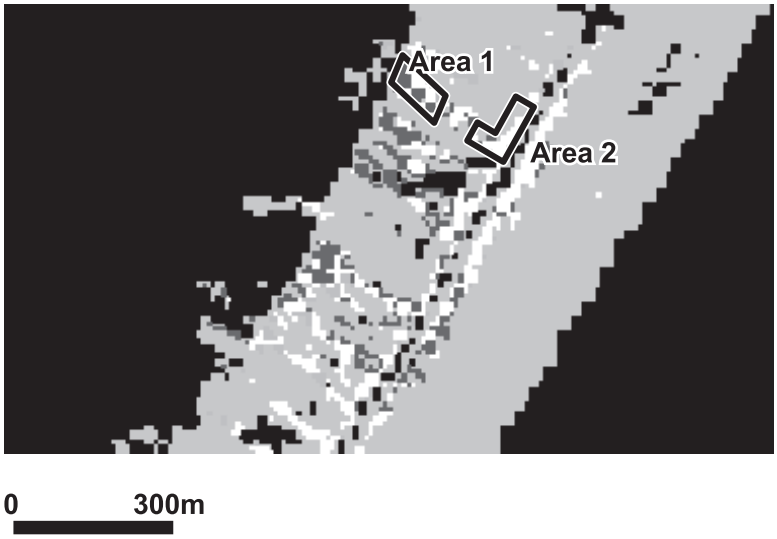

Figure 6. Composite image of 19 March-9 June NDVI differences data and 9 June-23 Nov NDVI differences data. R:G:B = 9 June-23 Nov NDVI differences data : 19 March-9 June NDVI differences data : 9 June-23 Nov NDVI differences data. Green area shows 19 March-9 June NDVI differences data > 0 and 9 June-23 Nov NDVI differences data : 0. Magenta area shows 19 March-9 June NDVI differences data : 0 and 9 June-23 Nov NDVI differences data > 0. White area shows 19 March-9 June NDVI differences data > 0 and 9 June-23 Nov NDVI differences data > 0.

Figure 7. Level of the 19 March-23 Nov NDVI differences on the 'No damage' coastal forest area after the tsunami.

the predominant class around them. This may arise from the mixel problem. In this case, a pixel contains a large other area than a pixel that is not influenced by the mixel problem, and hence, the pixel does not indicate the characteristics of the vegetation when there is a small decrease of NDVI. The influence of mixel is most likely to arise in areas at the boundary between coastal forest and other areas.

Conclusion

We analyzed middle spatial resolution satellite ALOS/AVNIR-2 and TERRA/ASTER data from the Tohoku coastal forest area, collected before and after the 11 March 2011 earthquake off the Pacific coast of Tohoku, and obtained the following results:

1. The damage to coastal forest immediately after the tsunami is assessed and classified into four classes

by unsupervised classification.

2. A relationship between the decrease in NDVI and the damage by 'Akagare' is revealed. 'Akagare' damage was found on 9 June and it has since expanded. The 'Akagare' damage was serious in the areas near the sea.

It is difficult to detect the distribution of damage in detail at an independent tree scale because of the mixel problem. However, in the case of a large-scale disaster like the 2011 Tohoku Earthquake, it is necessary to estimate the damage of a wide area quickly. The middle spatial resolution satellite with 10-15 m resolution can observe a 60-70 km swath width. It is valuable to detect the damage distribution of coastal forest immediately after the disaster and the progressive damage after the disaster.

Acknowledgments

We used ALOS/AVNIR-2 data provided by the Japan Aerospace Exploration Agency (JAXA), TERRA/ASTER data provided by the Geo GRID project team of the National Institute of Advanced Industrial Science and Technology. We would like to thank for them.

References

Alongi, D. M. (2008) Mangrove forests: Resilience, protection from tsunamis, and responses to global climate change. Estuarine, Coastal and Shelf Science, 76, 1:1-13.

Belward, A. S., H.-J. Stibig, H. Eva, F. Rembold, T. Bucha, A. Hartley, R. Beuchle, D. Khudhairy, M. Michielon and D. Mollicone (2007) Mapping severe damage to land cover following the 2004 Indian Ocean tsunami using moderate spatial resolution satellite imagery. International Journal of Remote Sensing, 28, 13-14: 977-2994.

Kathiresan, K. and N. Rajendran (2005) Coastal mangrove forests mitigated tsunami. Estuarine, Coastal and Shelf Science, 65: 601-606.

Kayaba, S. and S. Koshimura (2010) Mapping Tsunami Impact using Object-Based Satellite Image Analysis. Journal of Japan Society of Civil Engineers, Ser. B2 (Coastal Engineering), 66, 1: 1421-1425 (in Japanese).

Koshimura, S. and. H. Yanagisawa (2007) Developing fragility functions for tsunami damage estimation using the numerical model and satellite imagery, Proceedings of the 5th. International Workshop on Remote Sensing for Disaster Response.

Kouchi, K. and F. Yamazaki (2007) Characteristics of Tsunami-Affected Areas in Moderate-Resolution Satellite Images. IEEE Transactions on Geoscience and Remote Sensing, 45, 6:1650-1657.

Olwing, M. F., M. K. Sorensen, M. S. Rasmussen, F. Danielsen, V. Selvam, L. B. Hansen, L. Nyborg, K. B. Vestergaard, F. Parish and V. M. Karunagaran (2007) Using remote sensing to assess the protective role of coastal woody vegetation against tsunami waves. International Journal of Remote Sensing, 28, 13-14:3153-3169.

Sirikulchayanon, P., W. Sun and T. Oyana (2008) Assessing the impact of the2004 tsunami on mangroves using remote sensing and GIS techniques. International Journal of Remote Sensing, 29, 12:3553-3576.

Tanaka, N., Y. Sasaki, M. I. M. Mowjood, K. B. S. N. Jinadasa and S. Homchuen (2007) Coastal vegetation structures and their functions in tsunami protection: experience of the recent Indian Ocean tsunami. Landscape Ecol. Eng., 3: 33-45.

Tanaka, N. (2009) Vegetation bioshields for tsunami mitigation: review of effectiveness, limitations, construction, and sustainable management. Landscape Ecol. Eng., 5:71-79.

Taguchi, Y., N. Takagi, Y. Yamashita and H. Miyahara (2003) The analysis of the city Area albedo by a high resolution satellite data : research on the heat income and costs distribution map preparation in the city. Journal of the Remote Sensing Society of Japan, 23, 2: 147-156 (in Japanese).

Yanagisawa, H., S. Koshimura, K. Goto, T. Miyagi, F. Imamura, A. Ruangrassamee and C. Tanavud (2009) The reduction effects of mangrove forest on a tsunami based on field surveys at Pakarang Cape, Thailand and numerical analysis. Estuarine, Coastal and Shelf Science, 81: 27-37.